Paul R. Medwell Graham J. Nathana, Qing N. Chana, Zeyad T. Alwahabi, Bassam B. Dally
The influence of high intensity radiation on soot distribution within a laminar flame
Combustion and Flame, 2011; 158(9):1814-1821

Published at: http://dx.doi.org/10.1016/j.combustflame.2011.01.006

The influence of high intensity radiation on soot distribution within a laminar flame

Paul R. Medwell[a,c], Graham J. Nathan[a,c], Qing N. Chan[a,b,c], Zeyad T. Alwahabi[b,c], Bassam B. Dally[a,c]

[a] *School of Mechanical Engineering, The University of Adelaide, AUSTRALIA*
[b] *School of Chemical Engineering, The University of Adelaide, AUSTRALIA*
[c] *Centre for Energy Technology, The University of Adelaide, AUSTRALIA*

Abstract

An assessment of the influence of high intensity radiation on the distribution of soot within a laminar ethylene flame is performed. Radiation at fluxes of up to 4.3 MW/m^2, of a similar order encountered with concentrated solar radiation, is provided by a CO_2 laser at 10.6μm. Radiation at this wavelength, in the configuration used in this paper, allows isolation of three possible mechanisms of influence: molecular excitation of the fuel, irradiation of the soot, and irradiation of soot precursors. The influence of the radiation on the soot distribution is assessed by laser induced incandescence (LII) imaging in a plane that intersects with the CO_2 laser beam. It is found that the high intensity radiation has a dramatic influence on the flame. The high energy radiation acts to increase the peak volume fraction of the soot by up to 250%. The results show that whilst the effect is most pronounced due to heating of the fuel, heating of the soot can also be significant.

Keywords: Concentrated solar radiation, Laser Diagnostics, Soot, Coupled radiation heat transfer

1. Introduction

Combustion presently provides around 80% of the traded energy in industrialised economies and is expected to continue to be a major energy source for the foreseeable future [1]. At the same time, the need to mitigate the emissions of CO_2 is driving the development of technologies that utilise alternative energy sources, including solar energy [1]. Despite its many advantages and its potential to be the dominant source of sustainable energy in the long term, the use of Concentrated Solar Radiation (CSR) in thermal power generation remains significantly more expensive than many alternative energy sources [2, 3]. One approach to reduce the cost of solar thermal energy is to combine it with established technologies utilising fossil fuels. Such "hybrid" systems can typically halve the cost of solar thermal power, owing to the reduced infrastructure as well as potential thermodynamic synergies [4]. Traditional approaches to hybrid power generation technologies collect the thermal energy from the solar and combustion sources in separate devices and then combine them subsequently. However, a further reduction in infrastructure is possible by collecting these energy sources in the same device [5, 6]. Such processes result in the direct interaction of concentrated solar radiation on a flame or fuel. Solar concentrators can achieve radiant fluxes of 4,000 kW/m^2 [2]. This exceeds the natural radiation from most flames, which is already known to be sufficient to couple with combustion processes [7]. Hence there is a need to investigate the influence of high energy radiation on flames.

Radiation can interact with a flame via soot absorption, molecular excitation, or both. Soot particles absorb at all wavelengths of the solar spectrum, so will be heated by CSR to a higher temperature than the surrounding molecular gases. Due to this temperature difference ΔT ($\Delta T = T_{soot} - T_{gas}$) the energy will then be transferred to both the reactant and the oxidant gases, via the convection heat transfer process, and to the surrounding environment via radiation. The molecular excitation process can occur directly and/or indirectly. Direct excitation is a very efficient process, but is only possible if there is overlap of the molecule excitation spectrum and the wavelength of the incoming radiation. The indirect process is a two-step-process. In the first step, the incoming radiation is absorbed by molecules with high concentration, such as CO_2 and H_2O, making them vibrationally hot. In the second step, the energy will be transferred to both the reactant and the oxidant gases, via the inter-molecular energy transfer process. The relative strength of these interaction processes depends of the spectral characteristics of the fuel and the oxidant. Whichever the mechanism, sufficient heating of fuel molecules will stimulate their reaction, either of an oxidative or pyrolysis nature, depending on the stoichiometry. This paper focuses on radiation-flame interactions via both soot irradiation and the direct molecular excitation.

The direct energy transfer processes between high energy radiation and fuels have been given considerable attention in the production of nano-particles. This work has established that CO_2 lasers are an effective tool for providing direct energy transfer to ethylene (C_2H_4) via rotational and vibrational transitions [8], and that these can be very effective in promoting pyrolysis [9]. These findings provide a convenient starting point for the fundamental investigation of radiation-flame interactions, via the processes of direct molecular excitation and the broad-band heating of soot. They identify a unique combination of a readily available source of high power laser irradiation and a dominant and well-studied mechanism of molecular heating. Despite their differences, the use of CO_2 lasers allows a very great simplification over the extremely complex processes that would arise from the irradiation by a broad and non-uniform concentrated solar source.

Previous work has established that C_2H_4 has strong ro-vibrational transition overlapping the oscillating lines of a CO_2 laser around 10.6μm. It has also established that this process produces a wide range of hydrocarbon structures spanning aromatic compounds, PAH and other soot precursors through to carbon powders. It also reports the influence of laser power and pressure on absorption [8] and soot production [9] However, this previous work has been performed in specially designed pyrolysis reactors. No previous investigation has been performed to investigate the influence of intense radiation on the distribution and structure of a flame, including of the soot particles. Furthermore, such influences cannot be reliably predicted from available information because the processes of soot generation and radiation heat transfer are both non-linear and coupled. That is, an increase in the volume fraction of soot significantly reduces the flame temperature through increasing flame emissivity [10]. At the same time, the formation of soot also depends on temperature, T, in addition to fuel type and mixture fraction, ξ [11]. Similarly, its oxidation depends on T and on the strain rate in the reaction zone [10]. Since soot is preferentially distributed on the fuel-rich side of the local reaction zone [12], absorption of an external source of radiation by soot can be expected to preferentially increase temperatures in this region. The importance of such coupled processes has been well established in the related coupling processes between the natural radiation from a flame and turbulence [13, 7]. However, the coupling between externally introduced radiation and a flame is yet to be investigated.

To address these needs, the aim of the present work is to investigate the influence on the structure and distribution of soot in laminar flames, arising from the dual processes of soot irradiation and the direct molecular excitation. In particular it aims to assess the influence of the location of the irradiation source relative to the flame, and of the extent of pre-mixing of the fuel. This investigation is performed using a CO_2 laser as the source of irradiation and ethylene as the fuel, and its impact on flame structure is assessed via laser induced incandescence owing to the well-studied nature of this combination under pyrolysis conditions. This combination of laser and fuel enables a direct assessment of the role of direct molecular excitation, albeit at a different wavelength to solar radiation.

2. Experimental

2.1. Burner Details

The burner used in this study is a McKenna-type flat-flame burner, consisting of a porous stainless steel plug (⌀25mm). Non-premixed, partially premixed, or fully premixed ethylene/air laminar flames are studied, as shown in Table 1.

Note that in this paper the use of a stabilisation plate above the flat-flame, which is commonly used to prevent buoyancy-driven oscillation, was ***not*** employed. Soot Volume Fraction (SVF) images collected with such a plate in place clearly indicated negative effects of the plate by inducing recirculation of products back into the flame. No significant flame stability problems were noted in the absence of the stabilisation plate.

2.2. LII experimental details

The optical setup used for the present investigation is shown in Figure 1. The output of a multi-mode Nd:YAG laser at 1064 nm was used for laser-induced incandescence (LII) excitation. The laser beam was directed into a cylindrical-lens telescope with a horizontal axis to form a sheet of 50mm height. The thickness of the laser sheet was controlled by a cylindrical lens of a focal length of 1m with a vertical axis. The thickness of the sheet was measured to be ∼1mm through the measurement volume.

The operating LII fluence was 0.5 J/cm^2, which is within the plateau region (not shown here), to ensure that LII signals observed are independent of the laser fluence variation [14, 15]. The 'wings' of the nominally Gaussian laser sheet exhibiting low laser fluence were clipped with the use of a rectangular aperture.

The LII signal generated was detected through a 410nm optical filter (10 nm bandwidth), using an f-number 1.4 lens, onto an intensified CCD (ICCD) camera. The gate width of the camera was set to 100ns and the timing was set to be prompt to the LII excitation process to reduce the size-dependent sensitivity of the signal [16].

The LII measurements are calibrated via laser extinction. A chopped, continuous-wave 1064 nm beam was used to avoid absorption processes (from PAH or similar) [17, 18]. The soot extinction coefficient (K_e) was taken to be 9.2, following the work of Williams *et al.* [19].

The images presented have been corrected for background and detector attenuation (flat-field correction). The in-plane resolution of the images is 0.22mm per pixel. The images presented for this laminar flame system were median-averaged over 200 shots to improve on the SNR. Being a steady laminar flame, there is no loss of information resulting from the averaging. No pixel-binning was performed on the images to prevent degradation of the spatial resolution.

2.3. CO_2 experimental details

The output beam from a CO_2 continuous wave laser at 10.6μm was used as the source of high intensity irradiation to emulate the concentrated solar radiation (CSR) effect. In this paper we are simulating concentrated irradiation effects, and not aiming to use a CO_2 laser as a substitute for solar radiation. A CO_2 laser was chosen as it provides the most convenient source of continuous-wave controlled irradiation.

The laser output power is controlled via pulse-width modulation (PWM) was measured to have a maximum power output of 69W, with a stability of ±5%. The 10.6μm wavelength, 4.5mm diameter, beam was directed into the flame, at a slight (5.5°) angle to LII laser sheet. This small crossing-angle ensured overlap of the irradiation with the LII sheet throughout the measurement volume.

The use of a CO_2 laser to simulate solar radiation was chosen to provide a well-controlled source of CW radiation at the fluence of interest for concentrated solar radiation, namely 4.3 MW/m^2. It is noted that the use of a CO_2 laser will necessarily result in preferential absorption of CO_2 in the gas stream. Furthermore, the use of this wavelength will lead to intense absorption by the C_2H_4 fuel to enhance the interaction effects of the radiation source with the flame. However, the role of radiation interaction with soot in the flame will be essentially insensitive to the excitation wavelength through black-body absorption [19]. These two effects enable a separation of the influence on the soot distribution in the flame to be attributed to either direct molecular excitation or broadband absorption by the soot itself.

A comprehensive set of validation experiments were made to ensure the repeatability of the effects of the CO_2 laser irradiation. For the measurements presented in this paper, for the same flame condition, measurements were taken with/without irradiation immediately after one another.

3. Results

3.1. Effect of stoichiometry

Figures 2–5 present a series of planar images showing the distribution of soot volume fraction (SVF) in the laminar ethylene flame, either premixed, partially premixed or non-premixed. In each case, the distribution is shown both without (left) and with (right) the presence of a CO_2 laser-beam of consistent shape (4.5mm diameter), with fluence of 4.3 MW/m^2, and location of irradiation (height above burner, $HAB_{CO2} = 10mm$). Only the stoichiometry is changed from case to case.

Figure 2 presents the averaged images of the SVF for the ethylene/air flame premixed at a stoichiometry Φ=1.75 without (a) and with (b) the CO_2 laser irradiation. It is evident that the distribution of soot in the two images is qualitatively similar, but quantitatively different. The soot appears to be relatively uniformly distributed throughout the large central region of both flames. A comparison of the SVF levels in the two flames reveals that the CO_2

laser irradiation results in ∼66% increase in the magnitude of SVF at any given location. At this location, C_2H_4 from the source stream is consumed, hence this change is deduced to be predominantly attributable to the heating of soot and its precursors. In addition, both CO_2 and H_2O are present at this height and absorb at 10.6μm, so that molecular heating may also play a role. Through these absorptive processes, the temperature of the flame and reactants will be changed, thus influencing the chemistry and growth rate of soot, which are highly dependent on temperature [20, 21].

Attention is drawn to the location of the irradiation by the CO_2 laser beam, which is centred at a height of 10mm above the burner. Importantly, the influence of the CO_2 laser irradiation increases the SVF at all locations downstream from the source of irradiation, and not solely in the region of interaction. This shows that the time-scale of the influence is significantly longer than that of the physical interaction between the radiation and the combustion species.

Figure 3 presents the analogous images of SVF images for the non-premixed ethylene flame, again for the cases (a) without and (b) with the CO_2 laser irradiation. As for the premixed case (Figure 2), the SVF has been increased significantly by the CO_2 laser irradiation. However, the increase is even more significant, with the SVF increasing by 250%. Also like the premixed case, it is seen that the SVF increases at HAB values both within, and far downstream from, the interaction region between the flame and the irradiation. This additional increase in the SVF in the non-premixed case over the premixed flame is strongly suggestive of an increased role in the absorbtion of the CO_2 laser by the C_2H_4 fuel molecules; a process not occurring in the $\Phi = 1.75$ (Figure 2) flame due to the rapid consumption of fuel in the premixed configuration.

Worth noting is that the irradiation height is towards the base of the flame. At this location, the SVF is relatively low, so that absorption by soot is expected to play only a small role. This suggests that the dominant mechanism by which pyrolysis is promoted in this case is by the direct molecular heating of C_2H_4, as found in a pyrolysis reactor by Morjan *et al.* [9].

Figure 4 presents the equivalent averaged SVF images without and with irradiation for the case of a partially premixed flame, with Φ=3.76. In addition to the increase in SVF with the irradiation seen in the earlier figures, a broadening of the soot sheet towards the fuel-rich side is evident. Based on the lower level of C_2H_4 present in this flame (due to the partial premixing of the fuel stream) as compared with the non-premixed case, the absorption of the CO_2 laser by C_2H_4 is expected to be less. Despite the lower C_2H_4 concentration, a broader reaction zone is encountered in the Φ=3.76 flame, thus yielding CO_2 gases over a wider region in the flame as compared with the non-premixed case and therefore greater opportunity for the CO_2 gases to absorb the radiation. The combination of these effects are expected to lead to the less significant increase in the peak, but the broadening of the soot sheet under CO_2 laser irradiance. Further effect may occur through absorption of soot precursors.

Figure 5 presents the analogous image pairs of averaged SVF for a flame premixed to $\Phi = 1.94$. As with the previous cases, the SVF is found to increase with the irradiation, here with the peak increasing by 50%, and to also broaden the soot sheet. However, in addition, there is a qualitative difference in the shape. For the case without the CO_2 laser irradiation, the soot sheets on either side of the flame are quite distinct, and they only interact toward the top of the image. In contrast, the CO_2 laser irradiation causes the two sheets to clearly merge into a single soot sheet within the imaged region (although the SVF remains far from uniform). The significant upstream (downward) shift in the location at which soot is found on the axis of the burner indicates a very significant influence in the formation processes of the soot within the flame due by the CO_2 laser irradiation. The low volume fraction of soot or reactions at the location of the beam, particularly in the centre of the flame, implies that the effect of the irradiance is likely dominated through absorption by the C_2H_4 fuel.

Figure 6 compares the change in maximum volume fraction ($\Delta\mathrm{SVF}_{\mathrm{max}}$) and of the integrated soot volume fraction ($\Delta\mathrm{SVF}_{\mathrm{int}}$) within the sheet for all flames as a function of the extent of premixing. Here the increase is that for the case with the irradiation relative to that without the irradiation. The total is integrated only within the plane of the image since, even though the flame is cylindrical, the CO_2 laser irradiation is not axisymmetric and no information is available outside of the image plane. A consistent trend is evident, with the CO_2 laser irradiation causing a significant increase in the SVF (both peak and total) $\mathrm{SVF}_{\mathrm{max}}$ and $\mathrm{SVF}_{\mathrm{int}}$ to increase by $\sim$50%. However, there is a step change by a factor of about two in the influence as the mixture transitions from premixed to non-premixed. Indeed, the influence of premixing on $\Delta\mathrm{SVF}$ is relatively weak over the range explored here. Since the most significant increases in $\Delta\mathrm{SVF}$ are seen for the non-premixed flame, which has the highest C_2H_4 concentration, the step change is therefore attributable predominantly to the additional influence of the fuel pre-heating by molecular interaction. It is noted that the non-premixed flame also has the highest initial soot volume fraction, and therefore absorption of the irradiation via soot could also be used to justify why the non-premixed case gives the most significant increase. However, the changes in SVF between the non-premixed and premixed cases are much less pronounced than in C_2H_4 concentration, and the assertion is also supported by the high efficiency that C_2H_4 absorbs 10.6μm radiation.

3.2. Effect of laser irradiation height

Figures 7 & 8 present the average SVF image pairs for systematic variation in HAB_{CO2} using a similar format to that above. In each case, images are presented without and with the irradiation at 4.3 MW/m^2 from a CO_2 laser with all other parameters held constant.

Figure 7 presents the images for the non-premixed cases. It can be seen that the effect of the laser irradiation on the magnitude of SVF is most significant when the interaction height is near to the base of the flame. At this height the soot volume fraction is low, and therefore the increase in SVF is attributed largely to absorption of C_2H_4 molecules, or by soot precursors.

Figure 8 presents the analogous image pairs for the case Φ=3.76. These flames have a slightly broader reaction zone than the non-premixed case due to the additional air. It can be seen that, as with the non-premixed case presented in Figure 7, the irradiation at the downstream locations leads to a small, but still significant increase in the magnitude of SVF. The greatest influence is found at HAB_{CO2} = 10mm, where the SVF is found to increase by 29% and is also associated with a slight broadening of the soot sheet. In contrast, at HAB_{CO2} = 30mm no noticeable broadening occurs.

Figures 9 & 10 present radial profiles of SVF to assess the influence of the radiant heating on the magnitude and location of the soot sheet for the non-premixed and partially premixed ($\Phi = 3.76$) flames. In each case the radial profiles are obtained from 200-shot averages taken at 0mm, 5mm and 10mm downstream of the irradiation height at 10mm and 20mm HAB. The peak values in the profile confirm the trends already identified from the planar images and also reveal a number of other important details.

For the non-premixed flame heated near to the base of the flame at HAB_{CO2}=10mm, the influence is dramatic. At the same plane as the laser (HAB = HAB_{CO2} = 10mm), while the peak does not exhibit any significant change in magnitude, it causes a minor shift in the location of the peak towards the air stream. The shift in the location of the peak toward the lean side persists further downstream. For this condition the irradiation is found to cause an increase in SVF_{max} by a factor of 1.5 and 2.1 at HAB = 15 and 20mm respectively. The case HAB_{CO2} = 20mm exhibits similar trends, but to a lesser extent. In this case a significant shift in the radial location of the peak is only found further downstream at HAB=30mm. The peak also exhibits an increase by a factor of 30% at this height. These effects are likely due to the combined influences of direct molecular heating of the fuel and to the heating of soot and its precursors.

For the case of the partially premixed flame ($\Phi = 3.76$), the radial profile results indicate an increase in SVF only on the fuel rich side. The SVF_{max} increases by 25% and 30% at HAB = 15mm and 20mm, respectively, and in the thickness by around 50% and 75%, respectively based on the FWHM.

The shift of the soot sheet to the fuel-rich side is the opposite to what was observed for the non-premixed case. For the partially premixed flame, the shift is primarily observed only at the downstream locations, whereas for the non-premixed case the shift was noted at the same height as the irradiation.

3.3. Effect of irradiated CO_2 laser power

Figure11 presents the effect of varying the irradiation intensity on both SVF_{max} and SVF_{int} for the laminar non-premixed ethylene flame irradiated at HAB_{CO2} = 20mm. It can be seen that both the peak and total SVF remain approximately constant for laser power flux up to 3.4 MW/m^2. For power greater than this threshold the SVF is found to increase by 41.4% and 22.7% for the peak and total, respectively, between 0 and 4.3 $MW/^2$. The non-linearity seen in Figure 11 suggests that the mechanism of increase in SVF with laser power is highly sensitive to the heating exceeding a critical value.

4. Conclusions

This paper has presented the effects of concentrated radiation (using a CO_2 laser) on the soot volume fraction distribution in a range of ethylene (C_2H_4) flames. High energy irradiation, of a similar order encountered with concentrated solar radiation, has been used to assess three classes of influence on the structure and distribution of soot in a laminar flame. These are the direct molecular excitation of the C_2H_4, the irradiation of soot, and the irradiation of soot precursors. The combination of a CO_2 laser and C_2H_4 fuel has allowed a significant influence of each of these mechanisms to be achieved in a laminar flame. The variation of premixing has also been shown to allow the isolation of the influence of molecular heating of the fuel from that of the heating of the soot and its precursors, since ethylene is converted to other species by premixing within the region upstream from the zone of irradiation. The key findings associated with the assessment are as follows:

1. In all of the above three mechanisms, the time-scale of the effects are relatively long, with the greatest impacts being observed some 20mm downstream from the zone of irradiation. This is consistent with the relatively long time-scales of soot production.

2. The influence of the combined irradiation of fuel, soot and its precursors at an energy flux of 4.3 MW/m^2 and within a beam of 4.5mm diameter can lead to an increase in the peak soot volume fraction by up to 250%.

3. The mechanism found to exert the greatest influence on the maximum soot volume fraction is that of direct molecular excitation of the C_2H_4 fuel. Nonetheless, heating of the soot is also significant.

4. With partial premixing the influence of irradiation lead to a broadening of the soot region.

5. A lower-limit of radiation intensity was found to be necessary to achieve a significant influence on the irradiation of soot. A minimum intensity of 3.4 MW/m^2 through the same beam diameter of 4.5mm was found to be necessary to achieve a significant increase in SVF by irradiating the non-premixed flame at HAB_{CO2} = 20mm.

This work has highlighted a number of important issues relating to the soot formation process under concentrated irradiation. Future work, including detailed modelling and temperature measurement imaging using non-linear excitation regime two-line atomic fluorescence (NTLAF) [22, 23, 18, 24] is required to elucidate and extend the results presented in this paper.

References

[1] R. Sims, R. Schock, A. Adegbululgbe, J. Fenhann, I. Konstantinaviciute, W. Moomaw, H. B. Nimir, B. Schlamadinger, J. Torres-Martnez, C. Turner, Y. Uchiyama, S. J. V. Vuori, W. N., X. Zhang, Climate Change 2007: Mitigation. Contribution of Working Group III to the Fourth Assessment Report of the Intergovernmental Panel on Climate Change., Cambridge University Press, pp. 251–322.

[2] F. Kreith, D. Y. Goswami (Eds.), CRC Handbook of Energy Efficiency and Renewable Energy, Taylor and Francis Group, 2007.

[3] Sargent, Lundy, Assessment of Parabolic Trough and Power Tower Solar Technology Cost and Performance Forecasts, Technical Report Contract DE-AC36-99-GO10337, National Renewable Energy Laboratory, U.S. Department of Energy Laboratory, 2003.

[4] G. J. Kolb, Solar Energy 62 (1998) 51–61.

[5] A. Z'Grabben, P. Haueter, D. Trommer, M. Romero, J. C. de Jesus, A. Steinfeld, International Journal of Hydrogen Energy 31 (2006) 797–811.

[6] D. L. Battye, G. J. Nathan, P. J. Ashman, Solar Energy (2010) Submitted.

[7] P. J. Coelho, Progress in Energy and Combustion Science 33 (2007) 311–383.

[8] L. Giroux, M. H. Back, R. A. Back, Applied Physics B 49 (1989) 307–313.

[9] I. Morjan, I. Voicu, F. Dumitrache, I. Sandu, I. Soare, R. Alexandrescu, E. Vasile, I. Pasuk, R. M. D. Brydson, H. Daniels, B. Rand, Carbon 41 (2003) 2913–2921.

[10] B. F. Magnussen, B. H. Hjertager, Proceedings of the Combustion Institute 16 (1974) 719–727.

[11] K. M. Leung, R. P. Lindstedt, W. P. Jones, Combustion and Flame 87 (1991) 289–305.

[12] L. M. Pickett, J. B. Ghandhi, Combustion and Flame 132 (2003) 138–156.

[13] Y. Xin, J. P. Gore, K. B. McGrattan, R. G. Rehm, H. R. Baum, Combustion and Flame 141 (2005) 329–335.

[14] N. H. Qamar, Z. T. Alwahabi, Q. N. Chan, G. J. Nathan, D. Roekaerts, K. D. King, Combustion and Flame 156 (2009) 1339–1347.

[15] C. Schulz, B. F. Kock, M. Hofmann, H. Michelsen, S. Will, B. Bougie, R. Suntz, G. Smallwood, Applied Physics B 83 (2006) 333–354.

[16] R. L. Vander Wal, Applied Optics 35 (1996) 6548–6559.

[17] J. Zerbs, K. P. Geigle, O. Lammel, J. Hader, R. Stirn, R. Hadef, W. Weier, Applied Physics B 96 (2009) 683–694.

[18] Q. N. Chan, M. P. R., P. A. M. Kalt, Z. T. Alwahabi, B. B. Dally, G. J. Nathan, Proceedings of the Combustion Institute 33 (2010) In Press.

[19] T. C. Williams, C. R. Shaddix, K. A. Jensen, J. M. Suo-Anttila, International Journal of Heat and Mass Transfer 50 (2007) 1616–1630.

[20] S. T. Mauss, F., H. Bockhorn, Combustion and Flame 99 (1994) 697–705.

[21] J. Du, R. L. Axelbaum, Combustion and Flame 100 (1995) 367–375.

[22] P. R. Medwell, Q. N. Chan, P. A. M. Kalt, Z. T. Alwahabi, B. B. Dally, G. J. Nathan, Applied Optics 48(6) (2009) 1237–1248.

[23] P. R. Medwell, Q. N. Chan, P. A. M. Kalt, Z. T. Alwahabi, B. B. Dally, G. J. Nathan, Applied Spectroscopy 64(2) (2010) 173–176.

[24] Q. N. Chan, P. R. Medwell, P. A. M. Kalt, Z. T. Alwahabi, B. B. Dally, G. J. Nathan, Applied Optics 49(8) (2010) 1257–1266.

403 ## Tables and Tables captions

Flame Mode	Stoichimetry (Φ)
1	Non-premixed (∞)
2	3.76
3	1.94
4	1.75

Table 1: Table of ethylene flame conditions considered in this study

Figures and Figure captions

Figure Captions

Figure 1: Experimental Layout

Figure 2: (Color online) Averaged LII soot volume fraction images (a) without and (b) with 4.3 MW/m^2 irradiation at 10mm HAB (horizontal dashed line). Premixed ethylene/air flame, Φ=1.75. Note unique colour scale for each image.

Figure 3: (Color online) Averaged LII soot volume fraction images (a) without and (b) with 4.3 MW/m^2 irradiation at 10mm HAB (horizontal dashed line). Non-premixed ethylene. Note unique colour scale for each image.

Figure 4: (Color online) Averaged LII soot volume fraction images (a) without and (b) with 4.3 MW/m^2 irradiation at 10mm HAB (horizontal dashed line). Premixed ethylene/air flame, Φ=3.76. Note unique colour scale for each image.

Figure 5: (Color online) Averaged LII soot volume fraction images (a) without and (b) with 4.3 MW/m^2 irradiation at 10mm HAB (horizontal dashed line). Premixed ethylene/air flame, Φ=1.94. Note unique colour scale for each image.

Figure 6: Change in peak and integrated (over the image) SVF caused by the irradiation at 4.3 MW/m^2 as a function of stoichiometry.

Figure 7: (Color online) Averaged LII soot volume fraction images for non-premixed ethylene flames (a, c, e) without and (b, d, f) with 4.3 MW/m^2 irradiation at various height above burner (HAB). In each image pair, the bottom of the image is aligned 10mm below HAB_{CO2} (horizontal dashed line).

Note unique colour schemes for each image.

Figure 8: (Color online) Averaged LII soot volume fraction images for partially premixed ethylene flames with $\Phi = 3.76$ (a, c, e) without and (b, d, f) with 4.3 MW/m^2 irradiation at various height above burner (HAB). In each image pair, the bottom of the image is aligned 10mm below HAB_{CO2} (horizontal dashed line). Note unique colour schemes for each image.

Figure 9: (Color online) Averaged soot volume fraction radial profile for non-premixed flames, at two different laser irradiation heights (a) HAB_{CO2} = 10mm and (b) HAB_{CO2} = 20mm Circle: without laser irradiation. Dot: with laser irradiation.

Figure 10: (Color online) Averaged soot volume fraction radial profile for $\Phi = 3.76$, at two different laser irradiation heights (a) HAB_{CO2} = 10mm and (b) HAB_{CO2} = 20mm Circle: without laser irradiation. Dot: with laser irradiation.

Figure 11: (Color online) Peak and total SVF (integrated over image) as a function of laser power flux for the non-premixed case irradiated at HAB_{CO2} = 20mm.

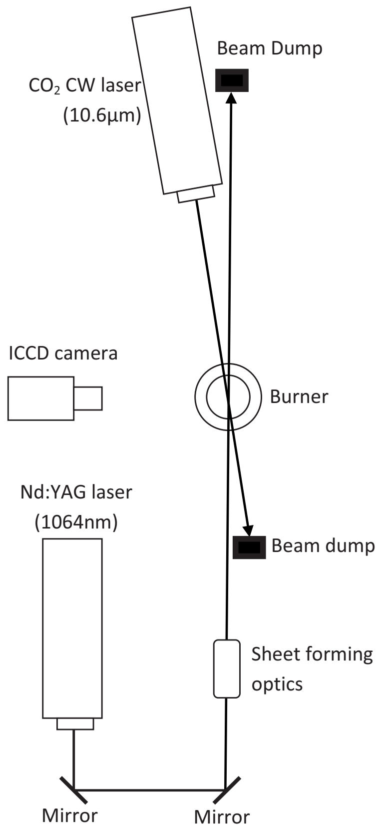

Figure 1: Experimental Layout

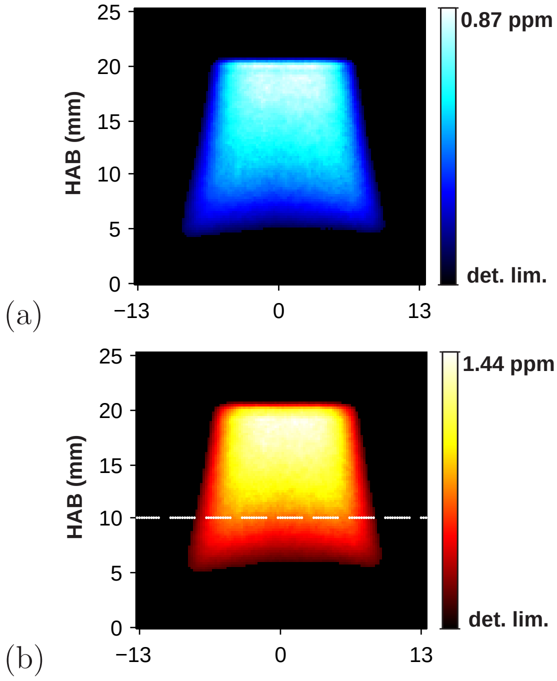

Figure 2: (Color online) Averaged LII soot volume fraction images (a) without and (b) with 4.3 MW/m^2 irradiation at 10mm HAB (horizontal dashed line). Premixed ethylene/air flame, Φ=1.75. Note unique colour scale for each image.

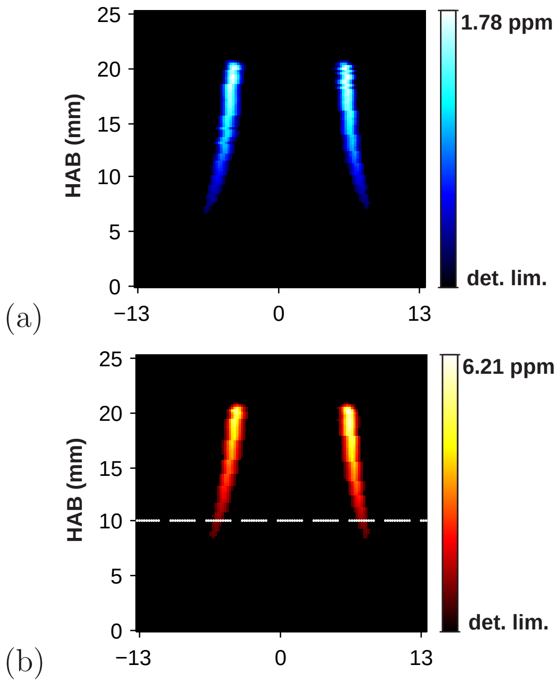

Figure 3: (Color online) Averaged LII soot volume fraction images (a) without and (b) with 4.3 MW/m^2 irradiation at 10mm HAB (horizontal dashed line). Non-premixed ethylene. Note unique colour scale for each image.

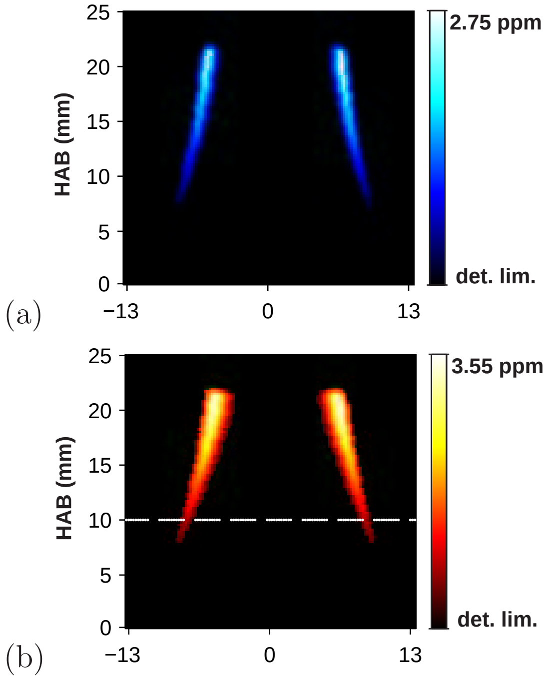

Figure 4: (Color online) Averaged LII soot volume fraction images (a) without and (b) with 4.3 MW/m^2 irradiation at 10mm HAB (horizontal dashed line). Premixed ethylene/air flame, Φ=3.76. Note unique colour scale for each image.

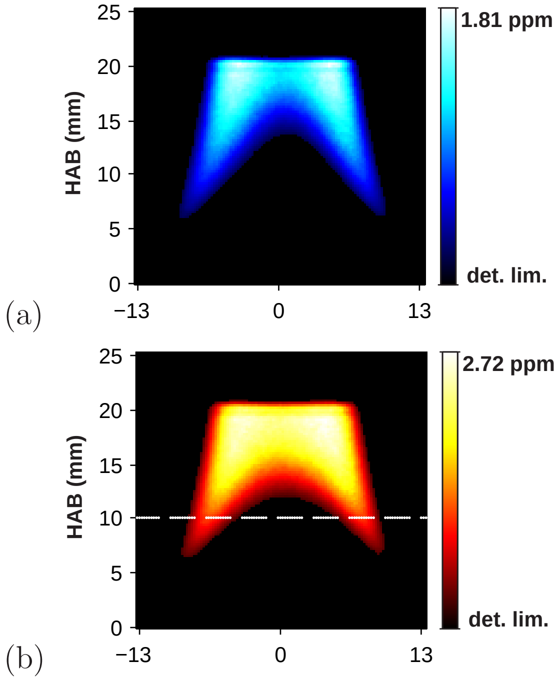

Figure 5: (Color online) Averaged LII soot volume fraction images (a) without and (b) with 4.3 MW/m^2 irradiation at 10mm HAB (horizontal dashed line). Premixed ethylene/air flame, Φ=1.94. Note unique colour scale for each image.

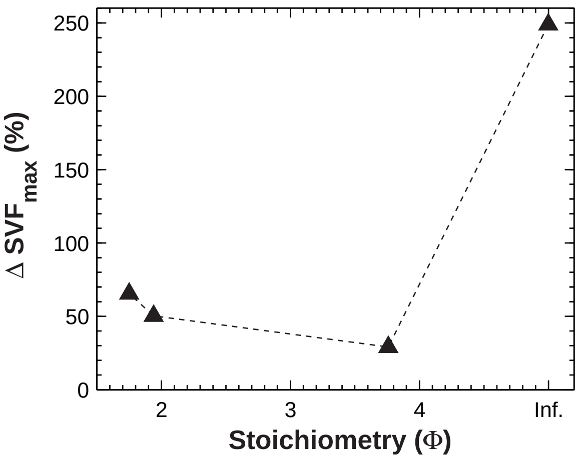

(a)

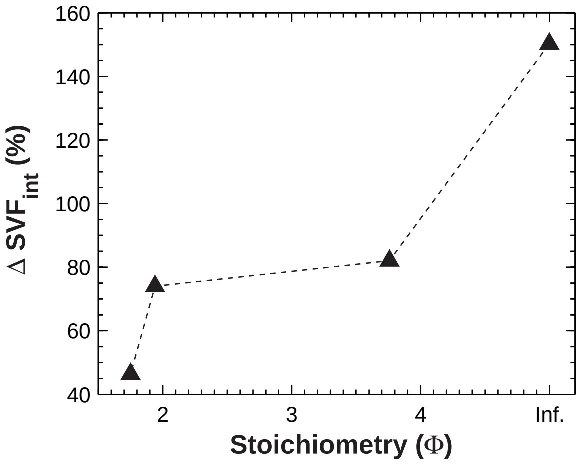

(b)

Figure 6: Change in peak and integrated (over the image) SVF caused by the irradiation at 4.3 MW/m^2 as a function of stoichiometry.

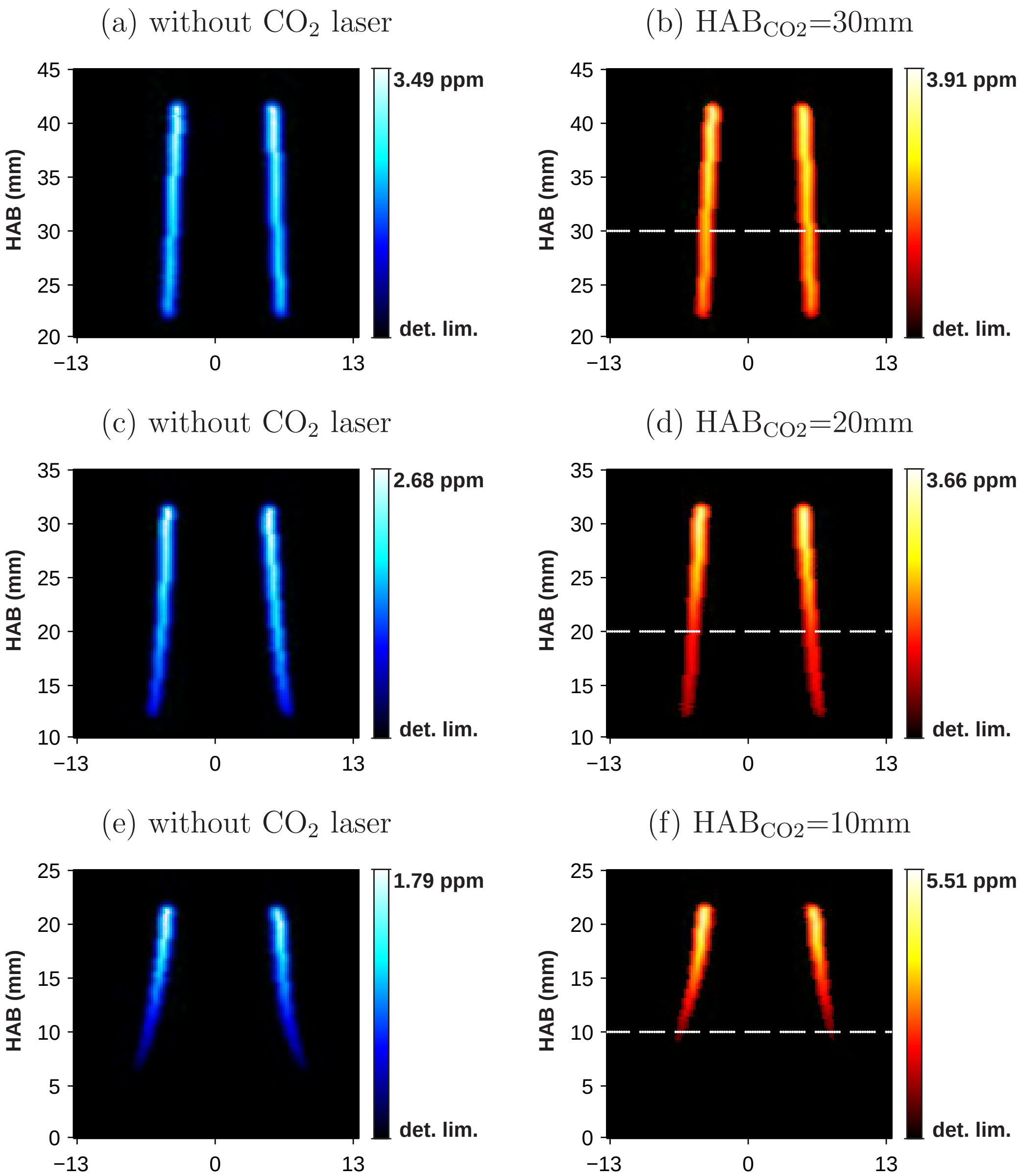

Figure 7: (Color online) Averaged LII soot volume fraction images for non-premixed ethylene flames (a, c, e) without and (b, d, f) with 4.3 MW/m^2 irradiation at various height above burner (HAB). In each image pair, the bottom of the image is aligned 10mm below HAB_{CO2} (horizontal dashed line). Note unique colour schemes for each image.

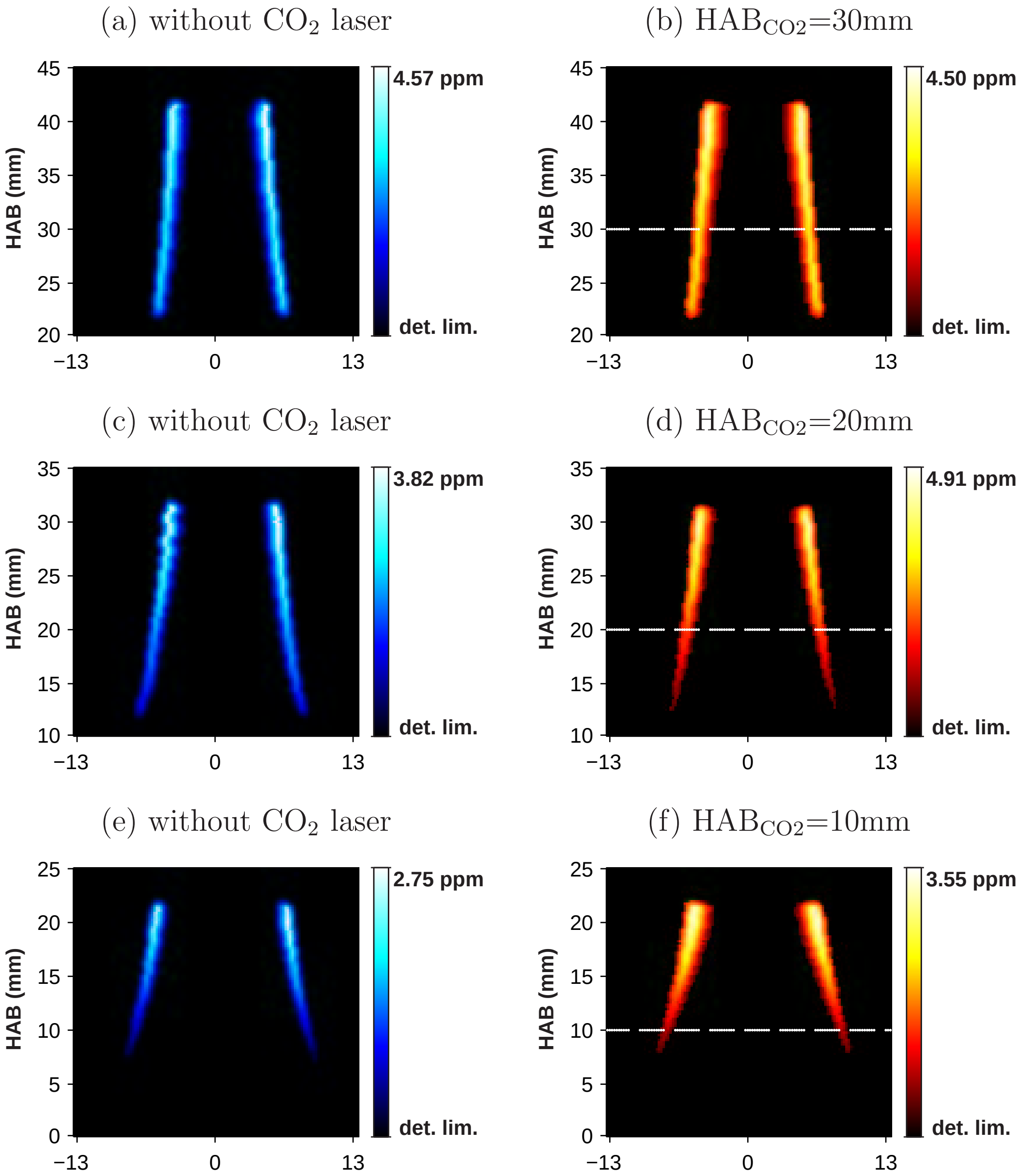

Figure 8: (Color online) Averaged LII soot volume fraction images for partially premixed ethylene flames with Φ = 3.76 (a,c,e) without and (b,d,f) with 4.3 MW/m^2 irradiation at various height above burner (HAB). In each image pair, the bottom of the image is aligned 10mm below HAB_{CO2} (horizontal dashed line). Note unique colour schemes for each image.

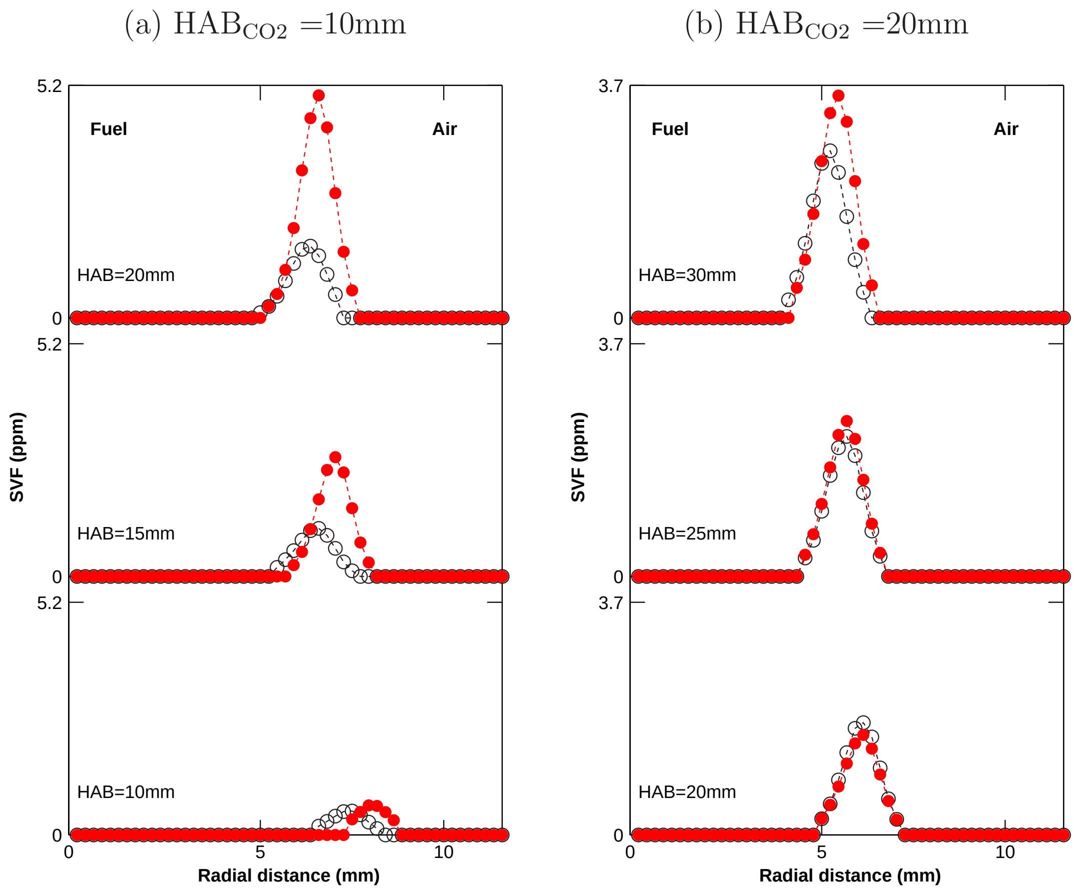

Figure 9: (Color online) Averaged soot volume fraction radial profile for non-premixed flames, at two different laser irradiation heights (a) HAB_{CO2} = 10mm and (b) HAB_{CO2} = 20mm Circle: without laser irradiation. Dot: with laser irradiation.

(a) HAB_{CO2} =10mm (b) HAB_{CO2} =20mm

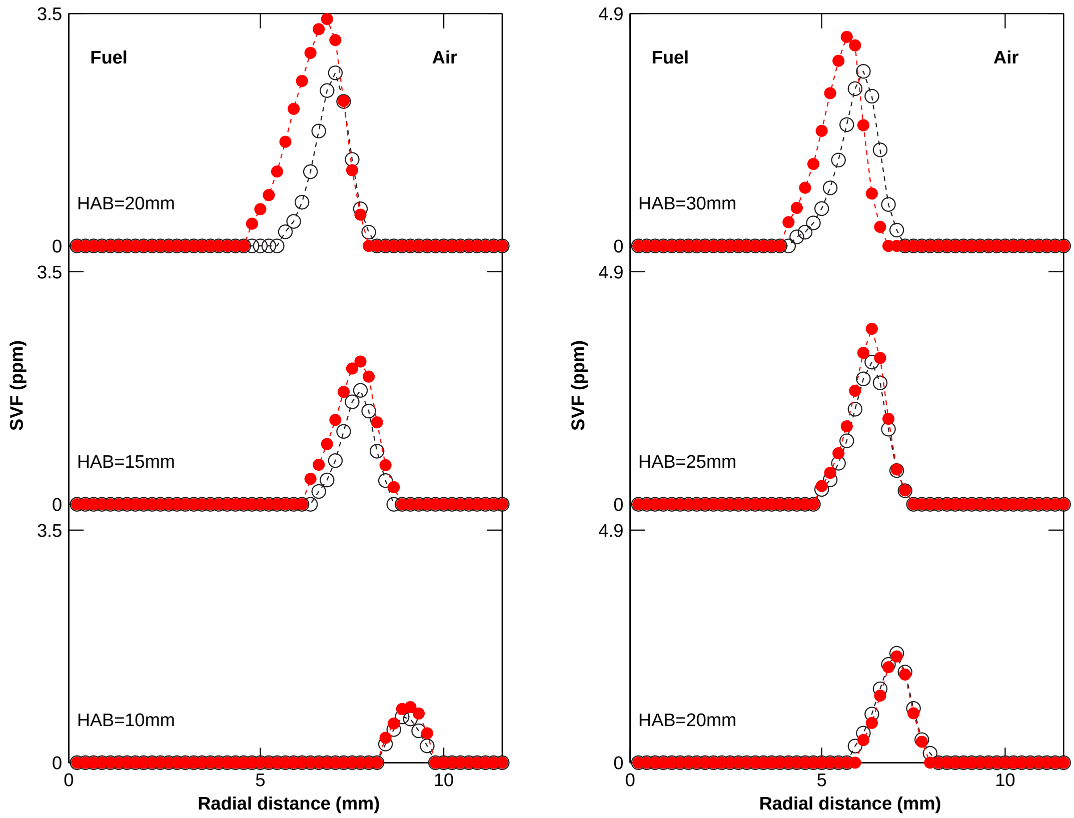

Figure 10: (Color online) Averaged soot volume fraction radial profile for $\Phi = 3.76$, at two different laser irradiation heights (a) $\text{HAB}_{\text{CO2}} = 10\text{mm}$ and (b) $\text{HAB}_{\text{CO2}} = 20\text{mm}$ Circle: without laser irradiation. Dot: with laser irradiation.

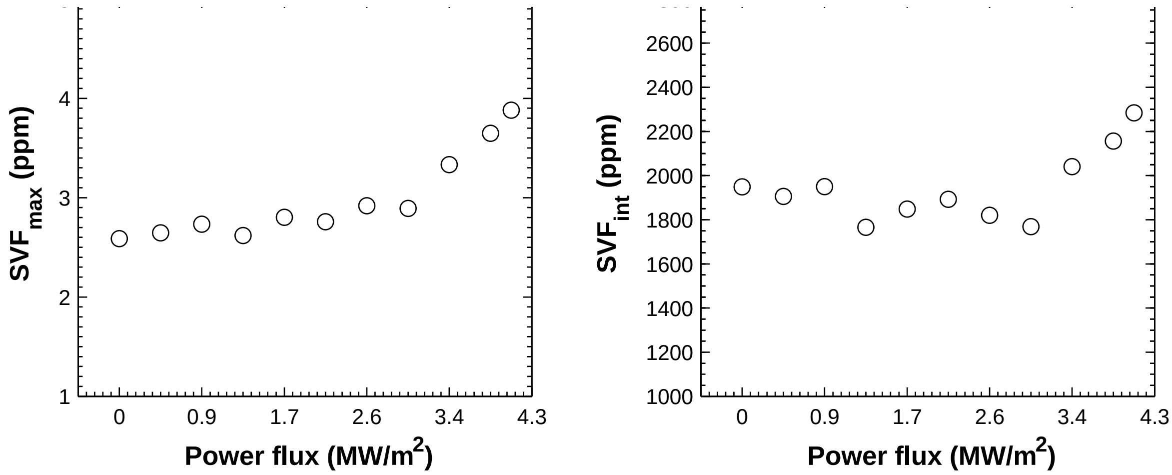

Figure 11: (Color online) Peak and total SVF (integrated over image) as a function of laser power flux for the non-premixed case irradiated at $\mathrm{HAB}_{\mathrm{CO2}} = 20\mathrm{mm}$.